Available online at www.sciencedirect.com
SCIENCE DIRECT
Tetrahedron 61 (2005) 9248–9256
Tetrahedron

Synthesis, X-ray crystallographic, and dynamic ^{1}H NMR studies of crown-tetrathia[3.3.3.3]metacyclophanes—conformational control by cooperative intramolecular C–H···π interaction both in solid state and in solution

Jian-Wei Xu,[a,b] Wei-Ling Wang[a] and Yee-Hing Lai[a,*]

[a]*Department of Chemistry, National University of Singapore, 3 Science Drive 3, Singapore 117543, Singapore*
[b]*Institute of Materials Research and Engineering, 3 Research Link, Singapore 117602, Singapore*

Received 11 May 2005; revised 6 July 2005; accepted 21 July 2005

Available online 11 August 2005

Abstract—Crown-tetrathia[3.3.3.3]metacyclophanes **3a–c** were synthesized via intermolcular coupling reaction in 22–30% yields. X-ray crystal analysis of **3b** revealed that it adopted a perpendicular conformation (**3b**-**B** or **3b**-**C**) in which two aromatic rings were inclined to be perpendicular to the opposite aromatic rings, driving two internal methyl groups into the π-cloud of the corresponding benzene rings. Furthermore, this perpendicular structural feature led to benzylic protons of thia-bridges being in close proximity to the adjacent aromatic rings. As a result, the induced upfield shifts for the two internal methyl protons and four benzylic protons were clearly observed in dynamic ^{1}H NMR spectra at low temperature, indicating that the intramolecular C–H···π interaction became increasingly important at low temperature. The energy barrier for inter-conversion between **3b**-**B** and **3b**-**C** was estimated to be 12.1 kcal mol^{-1} by using a coalescence method. The total stabilization enthalpy of the C–H···π interactions was quantitatively calculated to be 7.9 ± 0.8 kcal mol^{-1} by the dynamic NMR spectroscopy. In contrast, **3a** showed two non-interconvertible conformers at room temperature, which tended to interconvert at elevated temperature, however, many conformers co-existed at low temperature.

1. Introduction

The understanding of non-covalent weak interactions such as hydrogen-bonding, C–H···O/N, C–H···π, and N/O–H···π interactions, etc., is not only important in fundamental science, but also has implications for the development of various applications in crystal engineering and molecular design of materials.[1–7] Among these weak interactions, the C–H···π interaction, first explored by Nishio,[8–10] is considered as one of weak hydrogen bonds, in which the C–H and π-system acts as a soft acid and a soft base, respectively. The C–H···π interaction is of particular importance in influencing molecular recognition,[11–14] conformational preference,[15–24] biological processes, and the structure of biomacromolecules.[25–29] For example, Tsuzuki reported on the preferential conformation of crownophanes, which is determined by the co-effect of the C–H···π and C–H···O interactions.[15] Wilcox designed a sophisticated system to investigate the effect of the C–H···π interaction on molecular folding by using a 'slow rotation' strategy.[16–17] Ōki utilized the same strategy to take 1,9-disubstituted triptycenes as a model for the C–H···π interaction.[18–20] Additionally, many theoretical calculations[30–35] demonstrated that the C–H···π interaction is an attractive force in nature, and plays a role in stabilizing crystal packing.

The C–H and π-system in many organic molecules are in close proximity in crystalline state, however, it is sometime difficult to observe the C–H···π interaction in solution. This is because the mobility of a molecular structure usually results in conformationally averaged signals, for example, in the NMR spectra. Recently, as a parallel work of [*n*.3.3](1,2,6)cyclophanes,[36–37] we are focusing on the study of the synthesis, conformation, and complexation properties of [*n*.3.3](1,3,5)cycophanes.[38–39] Apart from the formation of cyclophanes as expected in the cyclization reaction, we isolated a dimeric product of a tetrathia[3.3.3.3]metacyclophane. X-ray single crystal analysis indicated that the intramolecular C–H···π interaction existed in solid state. Further dynamic NMR analysis revealed that cooperative intramolecular C–H···π (alkyl–aryl) interaction dominated

Keywords: Synthesis; Cyclophane; C–H···π Interaction; Conformation.
* Corresponding author. Tel.: +65 6874 2914; fax: +65 6779 1691; e-mail: chmlaiyh@nus.edu.sg

0040–4020/$ - see front matter © 2005 Elsevier Ltd. All rights reserved.
doi:10.1016/j.tet.2005.07.071

the conformation preference in solution, and its conformation at low temperature was similar to that in solid state. In the present paper, we report on their synthesis, X-ray structural characterization, and conformational behaviors of tetrathia[3.3.3.3]metacyclophanes.

2. Results and discussion

2.1. Synthesis of crown-tetrathia[3.3.3.3] metacyclophanes

The synthetic route leading to **3** is shown in Scheme 1. First, treatment of 2,4,6-trimethylphenol with a series of oligoethylene glycol dibromides in THF/NaOH solution afforded compounds **1a–c**. Bromomethylation of compounds **1a–c** in 47% hydrobromic acid/acetic acid and 1,3,5-trioxane using *N*,*N*,*N*-trimethyltetradecyl ammonium bromide as a phase transfer catalyst[40] was carried out to give tetrabromides **2a–c** in intermediate yields. As the reaction temperature was increased, the tribromide and tetrabromide gradually formed and their presence could be readily monitored by thin layer chromatography (TLC). Chromatography of the product mixture from the respective bromomethylation reactions gave **2a**, **2b**, and **2c** as white solids. In the ^{1}H NMR spectra of **2a**, **2b**, and **2c**, no aromatic proton signals were observed indicating that the aromatic positions in **1a**, **1b**, and **1c** were fully bromomethylated. When the tetrabromides **2a–c** were separately treated with 2 equiv of $Na_2S\cdot 9H_2O$ in 95% ethanol/benzene under high dilution conditions, a mixture of the intramolecularly coupled product[38] and the corresponding tetrathia[3.3.3.3]-metacyclophanes **3a–c** were obtained.

Taking the cyclization of **2b** as an example, the isolated product could in principle be any of **3b**, **4**, **5**, and **6**. The mass spectra of the compounds isolated from the cyclization of **2a–c** were determined using electrospray ionization (ESI) mass spectrometry. The isolated compound derived from **2a** showed molecular ions at 1027.5 ($[M+Na]^+$, 100). Similarly the compound derived from **2b** showed molecular ions at 1115.5 ($[M+Na]^+$, 30) and 1131.6 ($[M+K]^+$, 100) and that from **2c** at 1182.7 (M^+, 24), 1205.8 ($[M+Na]^+$, 14), and 1221.8 ($[M+K]^+$, 5). The above observation clearly confirmed that the corresponding compounds isolated were of dimeric nature. In the relatively simple ^{1}H NMR spectrum of **3b**, it appeared as three singlets at δ 2.47, 2.31, and 1.98 (integration ratio 1:1:1) corresponding to the three different pairs of methyl groups. This was further confirmed by a ^{13}C NMR DEPT experiment, which proved that there were three different types of methyl carbon signals at δ 14.86, 12.85, and 12.23, respectively, and two types of bridge carbon signals at δ 31.96 and 30.14. The above NMR data were collectively consistent with the structure of **3b** because the higher symmetry in **4**, **5**, or **6** should result in only two types of methyl protons or carbon signals. Although the ^{1}H NMR and ^{13}C NMR spectra of **3c** were very similar to those of **3b**, in particular the three types of protons and carbon NMR signals for the methyl groups, the spectra of **3a** were relatively more complicated. Compound **3a** showed six methyl protons signals in an integration ratio of 0.7:1:1:0.7:1:0.7 in CD_2Cl_2. This suggests the presence of two separate conformers that are non-interconverting in solution at room temperature. Additional evidence came from the 12 aromatic and four benzylic carbon signals observed in the ^{13}C NMR spectrum of the mixture (Fig. 1).

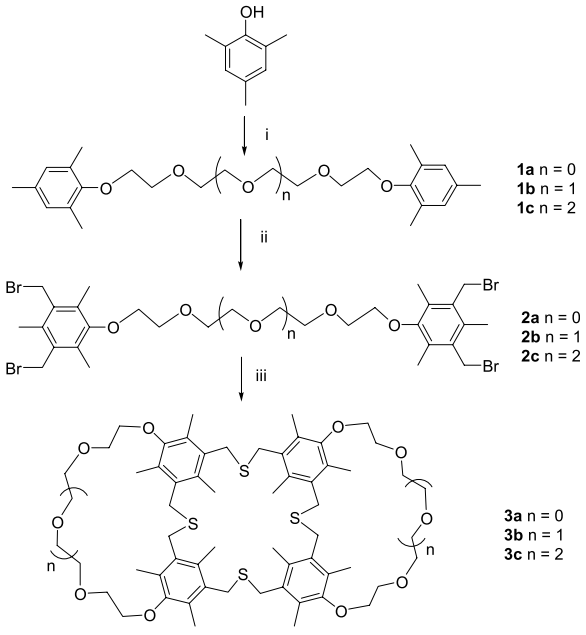

Scheme 1. The synthetic route for compounds **3a–c**. Reagents and conditions: (a) $Br(CH_2CH_2O)_nCH_2CH_2Br$, NaOH, THF; (b) 1,3,5-trioxane, HBr/HOAc, $C_{14}H_{29}N(CH_3)_3Br$; (c) Na_2S, Cs_2CO_3, C_2H_5OH/benzene.

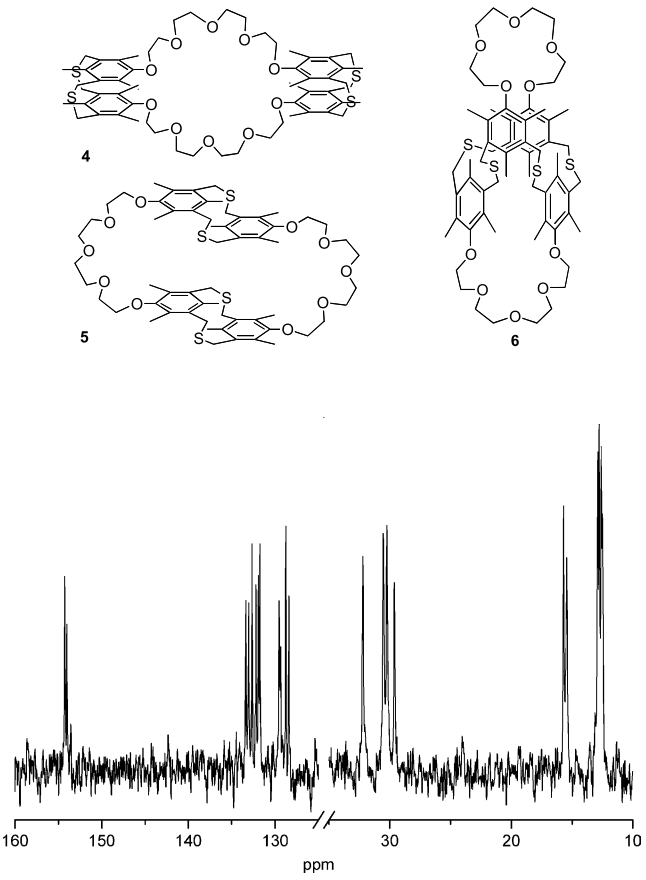

Figure 1. Part of ^{13}C NMR spectrum of compound **3a** in $CDCl_3$ at room temperature.

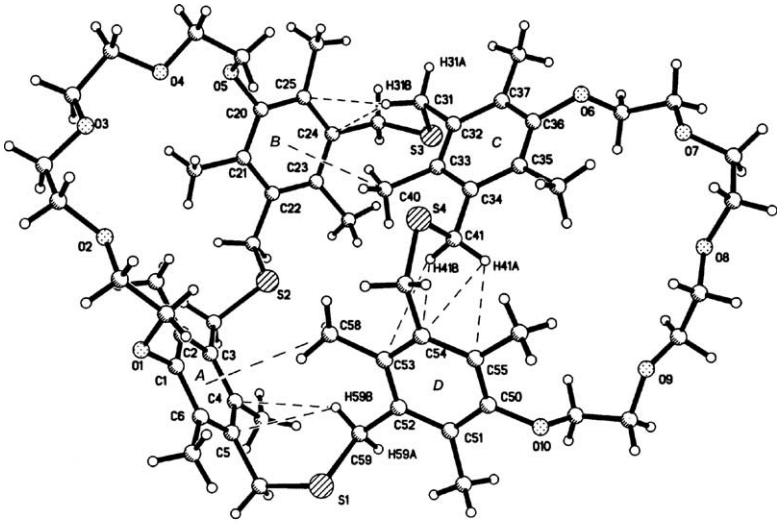

(a)

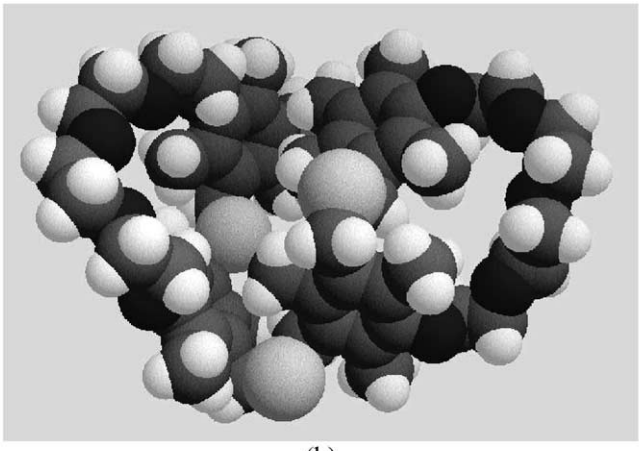

(b)

Figure 2. (a) ORTEP drawing of **3b** and (b) space-filling drawing of **3b** illustrating intramolecular close contacts.

2.2. X-ray crystallographic study of 3b

Single crystals of **3b** were grown by evaporative crystallization from a mixture of chloroform and acetonitrile solution, however, suitable crystals were not obtained for **3a** and **3c**. A drawing of the crystal structure of **3b** is shown in Figure 2. The four benzene rings (designated as A, B, C, and D in Fig. 2) in **3b** did not lie on the same plane as expected and each of them formed different dihedral angles (54.2° (ring B–ring A), 64.0° (ring C–ring D), 75.8° (ring B–ring C), and 71.7° (ring A–ring D)) with one another. The two oxa-crown macrorings were inclined to be approximately perpendicular to each other by bending the central thia-crown unit. Therefore, the whole molecule looked like an L-shape with two approximately perpendicular planes. In the crystal of **3b**, two internal methyl groups (C_{40} and C_{58}) were pointing toward the opposite aromatic rings B and A, respectively. The short distances (3.048 Å for C_{40}-ring A and 3.430 Å for C_{58}-ring B) between two internal methyl carbon atoms (C_{40} and C_{58}) and the geometrical centre of aryl rings (ring B and ring A) imply that they are subject to a C–H$\cdots\pi$ interaction (model a) as presented in Figure 3. Interestingly, four benzylic protons (H_{31B}, H_{41A}/H_{41B} and H_{59B}) are also in close proximity to the adjacent phenyl periphery (models b and c in Fig. 3). The distances between these benzylic protons concerned and C_{sp^2} of aromatic rings varied from 2.666 to 3.049 Å, being much shorter or approximately equal to that of van der Waals contact of H and C_{sp^2} (2.9–3.1 Å)[9] (Table 1). This type of C–H$\cdots\pi$ interaction is essentially comparable to the reported model,[33,41] in which the methylene group adopted a synclinal conformation, thus, leading to the methylene protons approaching the adjacent aromatic π-system.

It has been reported that the intramolecular edge–face aromatic interaction contributes to the stabilization of

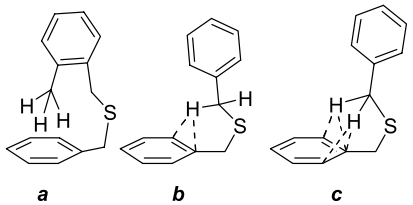

Figure 3. The intramolecular C–H$\cdots\pi$ interaction modes in **3b**.

Table 1. Non-bonded interatomic contacts (Å) and carbon···centroid distances in **3b**

Intramolecular contacts	Distance (Å)	Intramolecular contacts	Distance (Å)
H_{59B}–C_5	2.743	C_{59}–C_5	3.250
H_{59B}–C_4	2.764	C_{41}–C_{53}	3.545
H_{31B}–C_{24}	2.666	C_{41}–C_{54}	2.982
H_{31B}–C_{25}	2.713	C_{41}–C_{55}	3.459
H_{41A}–C_{55}	2.867	C_{31}–C_{24}	3.174
H_{41A}–C_{54}	2.795	C_{31}–C_{25}	3.451
H_{41B}–C_{54}	2.887	C_{40}–centroid	3.048[a]
H_{41B}–C_{53}	3.049	C_{58}–centroid	3.430[b]
C_{59}–C_4	3.545		

[a] The distances between C_{40} and geometric centre of ring A (C_1–C_2–C_3–C_4–C_5–C_6).
[b] The distance between C_{58} and geometric centre of ring B (C_{20}–C_{21}–C_{22}–C_{23}–C_{24}–C_{25}).

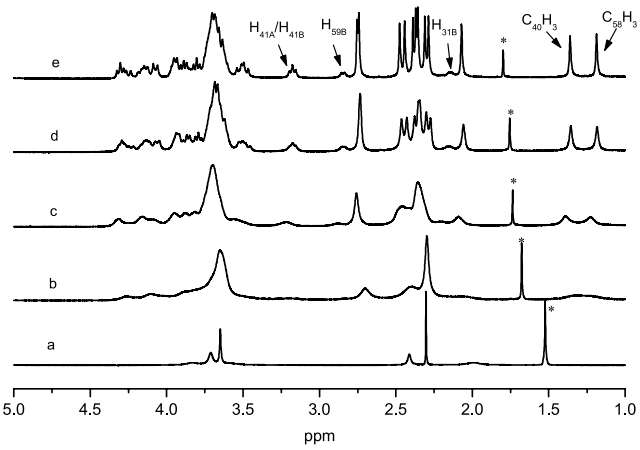

Figure 4. The variable-temperature ^{1}H NMR spectra of **3b** in CD_2Cl_2. (a) 298 K; (b) 253 K; (c) 243 K; (d) 233 K and (e) 223 K; *, residual water signal in CD_2Cl_2.

conformation of flexible molecules.[42] Similarly, intramolecular alkyl–aromatic interaction can perform the same role. This is because the methyl group possesses a three-fold axial symmetry and has more surface contact than aromatic edge–face interaction, which only has one interaction site. In fact the study of conformation population in the molecular folding reported by Wilcox has adduced the evidence that the intramolecular alkyl–aryl interaction has the same significance as the edge–face aromatic interaction in directing the conformation.[16–17] In general, intramolecular closeness between the C–H and π system results from the structural rigidity of a molecule, an attractive force between the C–H and π system or a consequence of crystal packing, which arises from the overall balance of interactions in a crystal structure. In the present case, the crowded structure of the C–H and the π system in **3b** does not come from intrinsic structural rigidity because **3b** can take non-congested conformations (see infra). The distances of C_{sp^2}–C_{sp^3} observed in **3b** was shorter than that of van der Waals contact for C_{sp^2}–C_{sp^3} by 4–19%. It seems persuasive that interactions (models a, b, and c in Fig. 3) are attributable to the stabilization of crystal packing. Taken together, these intramolecular cooperative C–H···π interactions would significantly exert a synergistic effect to force **3b** to take a perpendicular conformation in solid state.

2.3. Dynamic NMR spectroscopic study

Compound **3b**. As mentioned above, the close contacts between the C–H groups and π system in the solid state may stem from the attractive C–H···π interaction instead of crystal packing. However, in solution, if the C–H···π interaction observed functions effectively, **3b** is likely to prefer to a similar conformation to that in solid state when the effect of entropic factors on the conformation preference is reduced to an insignificant level at low temperature. For a flexible molecule, the conformation preference in solution is, however, pertinent to not only the enthalpic but also entropic factors due to the internal mobility[42] even though these C–H···π interactions are energetically attractive. Thus, in comparison with the conformation in solid state, **3b** was examined by ^{1}H NMR spectroscopy at 500 MHz over the temperature range of 298–223 K. (Fig. 4). At ambient temperature, the signals observed in ^{1}H NMR spectrum come from the averaged signals due to the dynamic equilibrium of all conformers. As the temperature decreased there were changes in their chemical shifts and they reappeared as four broad signals at δ 2.7, 2.4, 2.3, and 1.3, respectively. The signals began to sharpen at lower temperatures and at 223 K, 12 relatively sharp singlets with similar integration areas were observed for the methyl protons. It is particularly noteworthy that two substantially shifted signals emerged at δ 1.36 and 1.19. Meanwhile, three sets of signals at δ 3.17, 2.84, and 2.14 with an integration ratio of 2:1:1, which is very likely to correspond to benzylic protons namely H_{41A}/H_{41B}, H_{59B}, and H_{31B} (see Fig. 2a), respectively, were observed at the same temperature.

Considering the possible conformations with high symmetry, five different conformational structures of **3b** (Fig. 5) could correspond to that observed in the low temperature limit. These are **3b-A** (parallel), **3b-B** (perpendicular) or its mirror **3b-C**, **3b-D** (planar), and **3b-E** (stacked). The parallel conformer **3b-A** and planar conformer **3b-D** do not have any of its internal methyl groups lying within the shielding zone of another benzene ring and thus, should not have any significantly shielded methyl protons. Whereas a conformer like stacked **3b-E** is ruled out because it has all four internal methyl protons locating in the shielding zone of the opposite pair of aromatic rings. If the frozen conformation of **3b** were similar to that in the solid state as represented by perpendicular **3b-B** or **3b-C**, then there would be two shielded methyl proton signals that were consistent with what was observed. It was also observed that the three sets of benzylic signals were upfielded shift by ca. 0.47, 0.81, and 1.50 ppm[43] relative to that at room temperature. This concurs with the fact that the magnitude of upfield shifts observed correlates to the intra-atomic separation in solid state (H_{31B}–C_{sp^2} < H_{59B}–C_{sp^2} < H_{41A}(H_{41B})–C_{sp^2}), suggesting that the conformation in solution at low temperature agrees perfectly with that in solid state. Moreover, the ^{13}C NMR spectrum at 178 K might provide useful conformational information (Fig. 6). Two internal methyl carbons subjected to the C–H···π interaction downfielded shift by 0.45 and 1.57 ppm with respect to the chemical shifts at room temperature, while, another pair of internal methyl carbon without being

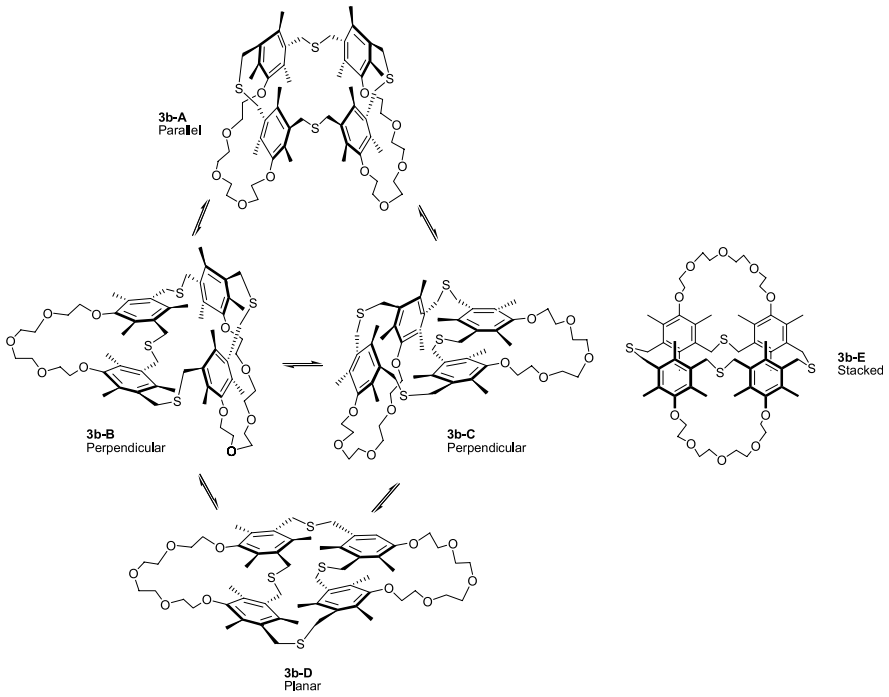

Figure 5. Possible conformation of **3b** in solution.

subjected to the C–H···π interaction experienced an upfielded shift of more than 1.57 ppm.

On the other hand, the inter-conversion between **3b**-**B** ⇔ **3b**-**C** would be established as the temperature was raised. The well-separated pair of significantly shielded methyl signals at high field served as the best probe in this conformational study. Using the Eyring equation,[44] the energy barrier ($\Delta G_c^{\neq}$) of inter-conversion between **3b**-**B** ⇔ **3c**-**C** was estimated to be about 12.1 kcal mol^{-1} (T_c=253 K, $\Delta\nu$=86 Hz).

As shown in Figure 4, all conformers convert rapidly on the NMR time scale at temperatures higher than 253 K. The chemical shifts of internal methyl protons are temperature dependent and are considered as weighted average signals, therefore, it is possible to estimate the enthalpy (ΔH°) and entropy (ΔS°) in terms of the following equations:[42,45]

$$\text{Observed internal methyl chemical shift} = P_1\delta_1 + 3(1-P_1)\delta_2$$

$$\text{Conformation with CH}-\pi\text{ interaction}\left(P_1\right) \overset{K}{\rightleftharpoons} \text{Conformation without CH}-\pi\text{ interaction}\left(1-P_1\right)$$

$$K = \frac{1-P_1}{P_1} = \exp\left[\frac{T\Delta S^\circ - \Delta H^\circ}{RT}\right]$$

Where P_1 is defined as the fractional population of conformers subject to C–H···π interaction and $1-P_1$ is the fractional population of conformers without C–H···π interaction. δ_1 and δ_2 represent the chemical shifts of internal methyl probe with or without C–H···π interaction, respectively. The calculated stabilization enthalpy and entropy are 7.9 ± 0.8 kcal mol^{-1} and 23 ± 3 cal mol^{-1}, respectively. The ΔH° is much larger than the contribution from a single C–H···π interaction (1.45 kcal mol^{-1})[31] and it is high enough to repel **3b** to take a complete perpendicular conformation as observed at low temperature at which the entropic effect was suppressed to a suitable low level. Therefore, we can conclude that in view of the enthalpy, the C–H···π interaction, which was amplified due to the cooperativity effect,[9–10,46] was responsible for the preferential conformation at low temperature.

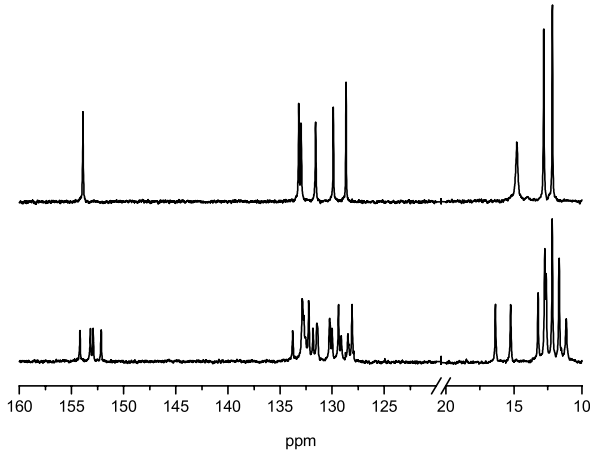

Figure 6. Part of the ^{13}C NMR spectrum of **3b** at 178 K. Top: 298 K and bottom: 178 K.

Compound **3a**. NMR analysis indicated two non inter-converting conformers of **3a** in solution at room temperature. It would thus, be interesting to determine whether they undergo inter-conversion at high temperature. The temperature-dependent ^{1}H NMR spectra of **3a** were measured in deuterated-nitrobenzene from room temperature to 393 K. As

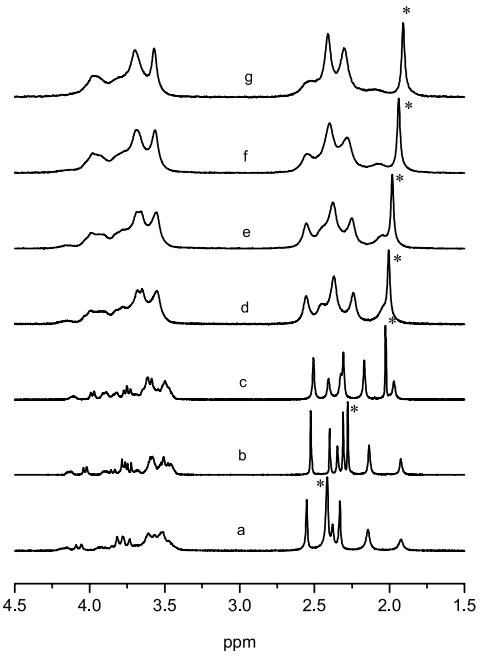

Figure 7. The variable-temperature ^{1}H NMR spectra of **3a** in deuterated nitrobenzene. (a) 300 K; (b) 315 K; (c) 352 K; (d) 368 K; (e) 373 K; (f) 383 and 393 K; *, residual water signal in deuterated nitrobenzene.

the temperature was raised to 393 K, the 12-methyl proton signals broadened and were partially overlapped to appear as four broad signals suggesting a possible inter-conversion between the two conformers or others (Fig. 7).

In contrast, the temperature-dependent ^{1}H NMR spectra of **3a** in CD_2Cl_2 were also determined down to the lower limit of 178 K (Fig. 8). At 300 K, the six methyl proton signals were resolved at δ 2.41, 2.31, 2.25, 2.13, 2.07, and 1.92, the last three being broad singlets. When the temperature was lowered, the three broad signals coalesced at about 273 K, and the other three began to broaden at about 253 K. At and below 233 K many new signals began to appear in the 'aromatic methyl proton' range. The spectra at the low temperature range were rather complicated and no peak

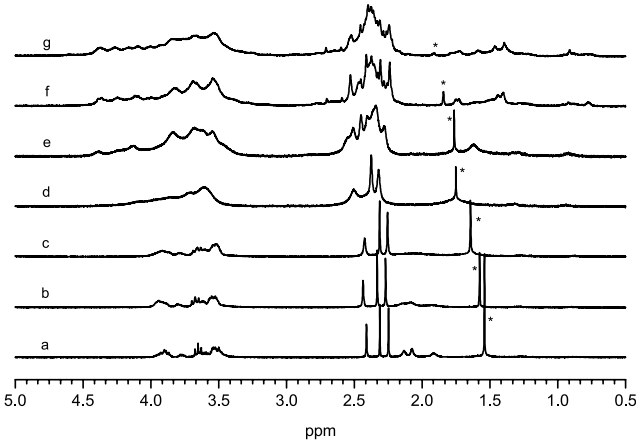

Figure 8. The variable-temperature ^{1}H NMR spectra of **3a** in CD_2Cl_2. (a) 298 K; (b) 283 K; (c) 273 K; (d) 253 K; (e) 233 K; (f) 193 K and (g) 178 K; *, residual water signal in CD_2Cl_2.

assignment or structural feature could be deduced, but the broad peaks around δ 1.40 in the NMR spectra at low temperature gave us an indication that the C–H$\cdots\pi$ interaction exists. The observation in general also indicated that the molecule **3a** could adopt many possible conformations at the low temperature limit but at room temperature two major conformers were present with a relatively high conformational barrier to inter-conversion.

3. Conclusions

In summary, crown-tetrathia[3.3.3.3]metacyclophanes were synthesized via cesium carbonate-assisted high dilution method with intermediate yields. X-ray crystallographic analysis of **3b** demonstrated that one pair of internal methyl groups was in close proximity to the opposite aromatic rings and, meanwhile, four benzylic protons approached the periphery of adjacent aromatic rings. The variable temperature NMR spectroscopic experiments showed that the chemical shifts of one pair of methyl groups and four benzylic protons were upfielded shift at low temperature. The change in chemical shifts intimated that the conformation in solution at low temperature was congruent to that observed in solid state. The correspondence in conformation between solid state and solution as well as the determination of total stabilization enthalpy of the C–H$\cdots\pi$ interaction revealed that the intramolecular cooperative C–H$\cdots\pi$ interaction dominated the preferential conformation both in solid state and in solution.

4. Experimental

4.1. General

All melting points were determined with a Sybron/Thermolyne MP-12615 melting point apparatus and were uncorrected. The ^{1}H NMR spectra were determined using $CDCl_3$ (unless otherwise stated) as solvent at room temperature on a Bruker ACF (300 MHz) or on a Bruker AMX (500 MHz) Fourier transform nuclear magnetic resonance spectrometer. All chemical shifts are reported in ppm downfield from tetramethylsilane as an internal standard. All ^{13}C NMR were determined in $CDCl_3$ at room temperature on a Bruker ACF (300 MHz) spectrometer. Infrared spectra were recorded on a Perkin-Elmer 1310 infrared spectrometer. Mass spectra were determined on a VG Micromass 7035 mass spectrometer at 70 eV with electron impact or on a Finnegan TSQ mass spectrometer with electrospraying ionization. Relative intensities are given in parenthesis. Microanalysis was performed by the Microanalytical Laboratory of the Department of Chemistry, National University of Singapore.

4.2. Preparation of compounds 1

General procedure. Sodium hydroxide (1.76 g, 44 mmol) was added to a solution of 2,4,6-trimethylphenol (6.0 g, 44 mmol) in THF (100 mL) to form the corresponding phenoxide ion. Oligoethylene glycol dibromide (22 mmol) was then added, and the mixture was stirred and refluxed overnight. After the reaction was complete, the THF in

mixture was removed under the reduced pressure, and then the residue was then poured into water and the product was extracted with dichloromethane. The organic layer was washed, dried, and evaporated. The crude product mixture was chromatographed on silica gel using ethyl acetate/hexane as eluent to give the desired product.

4.2.1. 1,8-Bis(2,4,6-trimethylphenoxyl)-3,6-dioxaoctane (1a). Yield: 64%; white solid: mp 98.5–100 °C; IR (KBr) 3005, 2923, 2895, 2874, 2857, 1486, 1453, 1365, 1322, 1307, 1275, 1236, 1215, 1135, 1041, 955, 904, 858, 783, 595 cm^{-1}. ^1H NMR δ 2.22 (6H, s, CH_3), 2.25 (12H, s, CH_3), 3.79 (4H, s, oxyethylene), 3.82–3.87 (4H, m, oxyethylene), 3.91–3.95 (4H, m, oxyethylene), 6.81 (4H, s, aromatic); MS (EI) *m/z* 386 (M^+, 69). Anal. Calcd for $C_{24}H_{34}O_4$: C, 74.58; H, 8.87. Found: C, 74.28; H, 9.10.

4.2.2. 1,11-Bis(2,4,6-trimethylphenoxyl)-3,6,9-trioxaundecane (1b). Yield: 83%; colorless oil; IR (neat) 3004, 2920, 2870, 2733, 1485, 1460, 1375, 1352, 1308, 1217, 1132, 1060, 1036, 955, 898, 855, 781 cm^{-1}. ^1H NMR δ 2.23 (6H, s, CH_3), 2.25 (12H, s, CH_3), 3.69–3.77 (8H, m, oxyethylene), 3.79–3.86 (4H, m, oxyethylene), 3.89–3.95 (4H, m, oxyethylene), 6.80 (4H, s, aromatic); MS (EI) *m/z* 430 (M^+, 58). Anal. Calcd for $C_{26}H_{38}O_5$: C, 72.53; H, 8.90. Found: C, 72.40; H, 8.74.

4.2.3. 1,14-Bis(2,4,6-trimethylphenoxyl)-3,6,9,12-tetraoxatetradecane (1c). Yield: 38%; pale yellowish oil; IR (neat) 3004, 2920, 2869, 1485, 1460, 1375, 1352, 1308, 1217, 1130, 1060, 955, 898, 855, 782 cm^{-1}. ^1H NMR δ 2.23 (6H, s, CH_3), 2.25 (6H, s, CH_3), 2.26 (6H, s, CH_3), 3.68–3.76 (12H, m, oxyethylene), 3.80–3.84 (4H, m, oxyethylene), 3.89–3.94 (4H, m, oxyethylene), 6.80 (4H, s, aromatic); MS (EI) *m/z* 474 (M^+, 62). Anal. Calcd for $C_{28}H_{42}O_6$: C, 70.86; H, 8.92. Found: C, 70.88; H, 8.79.

4.3. Preparation of compounds 2

General procedure. Compound **1** (7 mmol) was added to a mixture of 47% aq HBr (15 mL) and glacial acetic acid (100 mL), followed by 1,3,5-trioxane (4.8 g, 56 mmol) and tetradecyltrimethyl ammonium bromide (0.60 g). The mixture was warmed up and maintained at a temperature of 70 °C for 2 h followed by heating at 95–97 °C for 5 h (TLC was carefully performed to monitor the completeness of the reaction). After the reaction was complete, the reaction mixture was cooled to room temperature. The mixture was poured into ice-water and extracted with CH_2Cl_2. CH_2Cl_2 was washed with 5% $NaHCO_3$ and water, dried, and filtered. The organic solvent was removed under the reduced pressure and the residue was chromatographed on silica gel using ethyl acetate/hexane as eluent to afford **2**.

4.3.1. 1,8-Bis(2,4,6-trimethyl-3,5-dibromomethylphenoxyl)-3,6-dioxaoctane (2a). Yield: 54%; white solid: mp 147–149 °C; IR (KBr) 2923, 2874, 1457, 1309, 1263, 1208, 1109, 1052, 1020, 928, 873, 835, 628, 554 cm^{-1}. ^1H NMR δ 2.37 (12H, s, CH_3), 2.41 (6H, s, CH_3), 3.79 (4H, s, oxyethylene), 3.86 (8H, s, oxyethylene), 4.56 (8H, s, CH_2Br); MS (EI) *m/z* 754 (M^+, 0.3). Anal. Calcd for $C_{28}H_{38}Br_4O_4$: C, 44.35; H, 5.05. Found: C, 44.60; H, 4.79.

4.3.2. 1,11-Bis(2,4,6-trimethyl-3,5-dibromomethylphenoxyl)-3,6,9-trioxaundecane (2b). Yield: 68%; white solid: mp 131–134 °C; IR (KBr) 3004, 2925, 2870, 1456, 1417, 1379, 1346, 1308, 1263, 1208, 1138, 1105, 1051, 1017, 927, 871, 836, 792, 761, 704, 680, 628, 593, 570, 551, 467 cm^{-1}. ^1H NMR δ 2.36 (12H, s, CH_3), 2.40 (6H, s, CH_3), 3.75 (8H, s, oxyethylene), 3.85 (8H, m, oxyethylene), 4.55 (8H, s, CH_2Br); MS (EI) *m/z* 642 ($M^+ - 2^{79}Br$, 1). Anal. Calcd for $C_{30}H_{42}Br_4O_5$: C, 44.91; H, 5.28. Found: C, 45.30; H, 5.24.

4.3.3. 1,14-Bis(2,4,6-trimethyl-3,5-dibromomethylphenoxyl)-3,6,9,12-tetraoxatetradecane (2c). Yield: 59%; white solid: mp 114–116 °C; IR (KBr) 3005, 2949, 2874, 1455, 1420, 1377, 1348, 1309, 1263, 1208, 1141, 1118, 1108, 1072, 1052, 946, 872, 629, 553, 568, 468 cm^{-1}. ^1H NMR δ 2.36 (12H, s, CH_3), 2.40 (6H, s, CH_3), 3.70 (4H, s, oxyethylene), 3.71–3.77 (8H, m, oxyethylene), 3.80–3.88 (8H, m, oxyethylene), 4.55 (8H, s, CH_2Br); MS (EI) *m/z* 688 ($M^+ - 2Br$, 0.5). Anal. Calcd for $C_{32}H_{46}Br_4O_6$: C, 45.41; H, 5.48. Found: C, 45.42; H, 5.61.

4.4. Preparation of compounds 3

General procedure. A solution of 95% sodium sulfide nonahydrate (480 mg, 2.0 mmol) in 95% ethanol (300 mL) and a solution of tetrabromide **2** (1.0 mmol) in benzene (300 mL) in separate rotaflow dropping funnels were added dropwise simultaneously at the same rate to nitrogen purged 95% ethanol (1 L). After the addition the mixture was stirred for overnight and the bulk of the solvent was removed under reduced pressure. Water and dichloromethane were added to the residue, and the mixture was stirred until all solids dissolved. The organic layer was separated, dried, and evaporated. The residue was chromatographed on silica gel using ethyl acetate/hexane as eluent to give **3**.

4.4.1. 3,11,19,27-Tetrathia-7,15,23,31-biscrown-4-6,8,14,16,22,24,30,32,33,34,35,36,-dodecamethyl-[3.3.3.3]metacyclophane (3a). Yield: 22%; white solid: mp > 300 °C; IR (KBr) 2923, 2873, 1458, 1414, 1372, 1349, 1307, 1259, 1213, 1094, 933 cm^{-1}. ^1H NMR δ 1.91 (br s, CH_3), 2.10 (br s, CH_3), 2.13 (br s, CH_3), 2.26 (s, CH_3), 2.32 (s, CH_3), 2.39 (s, total integration for the six signals 36H with the relative intensities of the first, third, and fifth to the others being 0.7:1), 3.3–4.0 (m, 40H, CH_2S and oxyethylene); ^{13}C NMR δ 12.51, 12.61, 12.77, 12.90, 15.44, 15.71, 29.64, 30.24, 30.55, 32.24, 69.63, 70.41, 71.98, 72.14, 128.44, 128.77, 129.37, 129.55, 131.76, 131.93, 132.21, 132.67, 133.06, 133.39, 154.01, 154.26; MS (ESI) *m/z* 1005.5 ($[M+H]^+$, 15), 1027.5 ($[M+Na]^+$, 100). Anal. Calcd for $C_{56}H_{76}O_8S_4$: C, 66.89; H, 7.62. Found: C, 67.21; H, 7.90.

4.4.2. 3,11,19,27-Tetrathia-7,15,23,31-biscrown-5-6,8,14,16,22,24,30,32,33,34,35,36-dodecamethyl-[3.3.3.3]metacyclophane (3b). Yield: 30%; colorless crystal: mp 146–149 °C; IR (KBr) 2920, 2872, 1458, 1375, 1351, 1308, 1260, 1225, 1100, 936, 875, 731 cm^{-1}. ^1H NMR δ 1.98 (12H, br s, CH_3), 2.31 (12H, s, CH_3), 2.47 (12H, s, CH_3), 3.4–4.0 (48H, br m, CH_2S and oxyethylene); ^{13}C NMR δ 12.23, 12.85, 14.86, 30.14, 31.96, 70.25, 70.48, 70.93, 72.25, 128.75, 129.96, 131.66, 133.03, 133.26, 153.94; MS (ESI) *m/z* 1093.5 ([M+

H]$^+$, 4), 1131.6 ([M+K]$^+$, 100). Anal. Calcd for $C_{60}H_{84}O_{10}S_4$: C, 65.90; H, 7.74. Found: C, 65.63; H, 7.99.

4.4.3. 3,11,19,27-Tetrathia-7,15,23,31-biscrown-6-6,8,14,16,22,24,30,32,33,34,35,36,-dodecamethyl-[3.3.3.3]metacyclophane (3c). Yield: 30%; white solid: mp 194–197 °C; IR (KBr) 2916, 2868, 1458, 1420, 1373, 1351, 1309, 1260, 1242, 1100, 937, 877, 839 cm^{-1}. ^{1}H NMR δ 2.02 (12H, s, CH_3), 2.31 (12H, s, CH_3), 2.46 (12H, s, CH_3), 3.62–3.78 (56H, m, CH_2S and oxyethylene); ^{13}C NMR δ 12.00, 12.69, 14.61, 30.14, 31.93, 70.26, 70.70, 70.92, 71.16, 71.45, 72.02, 128.90, 129.67, 131.80, 132.78, 133.13, 153.43; MS (ESI) *m/z* 1181.7 ([M+H]$^+$, 35), 1203.7 ([M+Na]$^+$, 42). Anal. Calcd for $C_{64}H_{92}O_{12}S_4$: C, 65.05; H, 7.85. Found: C, 65.35; H, 8.00.

5. Supporting materials

Crystallographic data (excluding structure factors) for the structure in this paper has been deposited with the Cambridge Crystallographic Data Centre as supplementary publication numbers CCDC 186822 (**3b**). Copies of the data can be obtained, free of charge, on application to CCDC, 12 Union Road, Cambridge CB2 1EZ, UK [fax: +44 1223 336033 or e-mail: deposit@ccdc.cam.ac.uk].

Acknowledgements

We are grateful to the National University of Singapore (NUS) for financial support. Assoc Prof. J. J. Vittal and Ms. Tan Geok Kheng are acknowledged for determining the X-ray crystallographic structures in the X-ray diffraction laboratory at the Department of Chemistry, NUS.

References and notes

1. Holman, K. T.; Pivovar, A. M.; Ward, M. D. *Science* **2001**, *294*, 1907–1911.
2. Muthuraman, M.; Masses, R.; Nicoud, J.-F.; Desiraju, G. R. *Chem. Mater.* **2001**, *13*, 1473–1479.
3. Debrus, S.; Ratajczak, H.; Venturini, J.; Pincon, N.; Baran, J.; Barycki, J.; Glowiak, T.; Pietraszko, A. *Synth. Met.* **2002**, *127*, 99–104.
4. Guru, R. T. N. *Coord. Chem. Rev.* **1999**, *183*, 81–100.
5. Thalladi, V. R.; Brasselet, S.; Weiss, H.-C.; Blaeser, D.; Katz, A. K.; Carrell, H. L.; Boese, R.; Zyss, J.; Nangia, A.; Desiraju, G. R. *J. Am. Chem. Soc.* **1998**, *120*, 2563–2577.
6. Rovira, C. *Chem. Eur. J.* **2000**, *6*, 1723–1729.
7. Cole, J. M.; Howard, J. A.; Mclntyre, G. J. *Acta Crystallogr. Sect. B Struct. Sci.* **2001**, *57*, 410–414.
8. Kodama, Y.; Nishihata, K.; Nishio, M. *Tetrahedron Lett.* **1977**, *24*, 2105–2108.
9. Nishio, M.; Hirota, M. *Tetrahedron* **1989**, *45*, 7201–7245.
10. Nishio, M.; Hirota, M.; Umezawa, Y. *The CH/pi Interaction: Evidence, Nature, and Consequences*; Wiley-VCH: New York, 1998.
11. Nishio, M.; Umezawa, Y.; Hirota, M.; Takeuchi, Y. *Tetrahedron* **1995**, *51*, 8665–8701.
12. Amabilino, D. B.; Ashton, P. R.; Brown, C. L.; Córdova, E.; Godínez, L. A.; Goodnow, T. T.; Kaifer, A. E.; Newton, S. P.; Pietraszkiewicz, M.; Philp, D.; Raymo, F. M.; Reder, A. S.; Rutland, M. T.; Slawin, A. M. F.; Spencer, N.; Stoddart, J. F.; Williams, D. J. *J. Am. Chem. Soc.* **1995**, *117*, 1271–1293.
13. Frontera, A.; Garau, C.; Quionero, D.; Ballerster, P.; Costa, A.; Deya, P. M. *Org. Lett.* **2003**, *5*, 1135–1138.
14. Amabilino, D. B.; Ashton, P. R.; Stoddart, J. F.; Menzer, S.; Williams, D. J. *J. Chem. Soc., Chem. Commun.* **1994**, 2475–2478.
15. Tsuzuki, S.; Houjou, H.; Nagawa, Y.; Hiratani, K. *J. Chem. Soc., Perkin Trans. 2* **2001**, 1951–1955.
16. Kim, E.; Paliwal, S.; Wilcox, C. S. *J. Am. Chem. Soc.* **1998**, *120*, 11192–11193.
17. Paliwal, S.; Wilcox, C. S. *J. Am. Chem. Soc.* **1994**, *116*, 4497–4498.
18. Ōki, M. *Acc. Chem. Res.* **1990**, *23*, 351–356.
19. Nakai, Y.; Yamamoto, G.; Ōki, M. *Chem. Lett.* **1987**, 89–92.
20. Nakai, Y.; Inoue, K.; Yamamoto, G.; Ōki, M. *Bull. Chem. Soc. Jpn.* **1989**, *62*, 2923–2931.
21. Umezawa, Y.; Tsuboyama, S.; Takahashi, H.; Uzawa, J.; Nishio, M. *Tetrahedron* **1999**, *55*, 10047–10056.
22. Kitahara, Y.; Tanaka, K. *J. Chem. Soc., Chem. Commun.* **2002**, 932–933.
23. Yoshitake, Y.; Misaka, J.; Setogushi, K.; Abe, M.; Kawaji, T.; Eto, M.; Harano, K. *J. Chem. Soc., Perkin Trans. 2* **2002**, 1611–1619.
24. Matsugi, M.; Itoh, K.; Nojima, M.; Hagimoto, Y.; Kita, Y. *Tetrahedron Lett.* **2001**, *42*, 6903–6905.
25. Nishio, M.; Umezawa, Y.; Tsuboyama, S.; Takahashi, H.; Uzawa, J. *Pept. Sci.* **1999**, *36*, 61–64.
26. Chakrabarti, P.; Samanta, U. *J. Mol. Biol.* **1995**, *251*, 9–14.
27. Umezawa, Y.; Nishio, M. *Bioorg. Med. Chem.* **1998**, *6*, 493–504.
28. Umezawa, Y.; Nishio, M. *Bioorg. Med. Chem.* **2000**, *8*, 2643–2650.
29. Muraki, M. *Protein Pept. Lett.* **2002**, *9*, 195–209.
30. Bagno, A.; Saielli, G.; Scorrano, G. *Chem. Eur. J.* **2002**, *8*, 2047–2056.
31. Tsuzuki, S.; Honda, K.; Uchimaru, T.; Mikami, M.; Tanabe, K. *J. Am. Chem. Soc.* **2000**, *122*, 3746–3753.
32. Takahashi, O.; Kohno, Y.; Gondoh, Y.; Saito, K.; Nishio, M. *Bull. Chem. Soc. Jpn.* **2003**, *76*, 369–374.
33. Takahashi, O.; Kohno, Y.; Saito, K.; Nishio, M. *Chem. Eur. J.* **2003**, *9*, 756–762.
34. Ugozzoli, F.; Arduini, A.; Massera, C.; Pochini, A.; Secchi, A. *New J. Chem.* **2002**, *26*, 1718–1723.
35. Ribas, J.; Cubero, E.; Luque, F. J.; Orozco, M. *J. Org. Chem.* **2002**, *67*, 7057–7065.
36. Xu, J.-W.; Lai, Y.-H. *Org. Lett.* **2002**, *4*, 3211–3214.
37. Xu, J.-W.; Lai, Y.-H. *Tetrahedron Lett.* **2002**, *43*, 9199–9202.
38. Xu, J.-W.; Lai, Y.-H.; Wang, W.-L. *Org. Lett.* **2003**, *5*, 2781–2784.
39. Xu, J.-W.; Lin, T.-T.; Lai, Y.-H. *Tetrahedron* **2005**, *61*, 2431–2440.
40. Mitchell, R. H.; Iyer, V. S. *Synlett* **1989**, 55–57.
41. Sicher, J.; Cherest, M.; Gault, Y.; Felkin, H. *Collect. Czech. Chem. Commun.* **1963**, *28*, 72–81.
42. Jennings, W. B.; Farrell, B. M.; Malone, J. F. *Acc. Chem. Res.* **2001**, *34*, 885–894.
43. The changes in chemical shift were approximately estimated based on δ=3.65 for benzylic protons at room temperature.
44. Calder, I. C.; Garratt, P. J. *J. Chem. Soc. B* **1967**, 660–662.

45. The chemical shifts for internal methyl protons are calculated according to the modified method. At equilibrium, three pairs of internal methyl groups locate the unshielded zone, while, only one pair of methyl groups lie in the shielded zone. Thus, observed chemical shift for internal methyl protons is given by $P_1\delta_1+3(1-P_1)\delta_2$. For examples on the quantitative measurement of enthalpy per C–H$\cdots\pi$ interaction, also see: Ehama, R.; Yokoo, A.; Tsushima, M.; Yuzuri, T.; Suezawa, H.; Hirota, M. *Bull. Chem. Soc. Jpn.* **1993**, *66*, 814–818.
46. Steiner, T. *J. Chem. Soc., Chem. Commun.* **1995**, 95–96.